

Synthesis and Properties of Oligothymidylates Incorporating an Artificial Bend Motif

by Kohji Seio, Takeshi Wada, and Mitsuo Sekine*

Department of Life Science, Faculty of Bioscience and Biotechnology, Tokyo Institute of Technology,
Nagatsuta, Midori-ku, Yokohama 226-8501, Japan

Dedicated to Prof. Dr. *Frank Seela* on the occasion of his 60th birthday

The uridylyl-(3' → 5')-thymidine dinucleotide block **14** (cUpdU), having a cyclic structure between the 2'-hydroxy of the upstream uridine and the 5-substituent of the downstream thymidine, was synthesized (*Schemes 1* and *2*). This cyclic structure is a stable mimic of the intraresidual H-bonding found in the anticodon loop of an *E. coli* minor tRNA^{Asp}. The spectroscopic and molecular-mechanics analyses of the cyclized dinucleotides predicted two major conformers, *i.e.*, the turn and bent forms. The latter was expected to bend DNA oligomers when incorporated into them. This expectation was ascertained by incorporating the bent dimer motif into tetra-, deca-, or hexadecathymidylates by the conventional phosphoramidite method (see **18–20** in *Scheme 4*). The bending of oligonucleotides **18–20** was demonstrated by ³¹P-NMR and CD spectra and gel-electrophoretic studies. The duplex formation of these modified oligonucleotides with oligodeoxyadenylates was also studied. The decreased thermal stability of the duplexes when compared with unmodified ones indicates distorted structures of the modified duplexes. The 3D computer model of the duplexes showed a bend of *ca.* 30° with a 'bulge-out' at the position of an adenosine residue facing the cyclized dimer. The artificially bent DNAs might become a new tool for the study of the effect of DNA bending induced in DNA/DNA-binding protein interactions.

1. Introduction. – DNA Bending induced by DNA-binding proteins (DBP) is an important event in a series of biological reactions related to the expression, recombination, and replication of genetic information [1]. The detailed tertiary structures of some bent DNAs have been unveiled to date with the aid of X-ray crystallographic or multi-dimensional NMR spectroscopic techniques [1]. Sharply bent structures have also been discovered in the active site of hammerhead ribozymes [2] as well as in the region between the anticodon and its upstream nucleoside in tRNA [3].

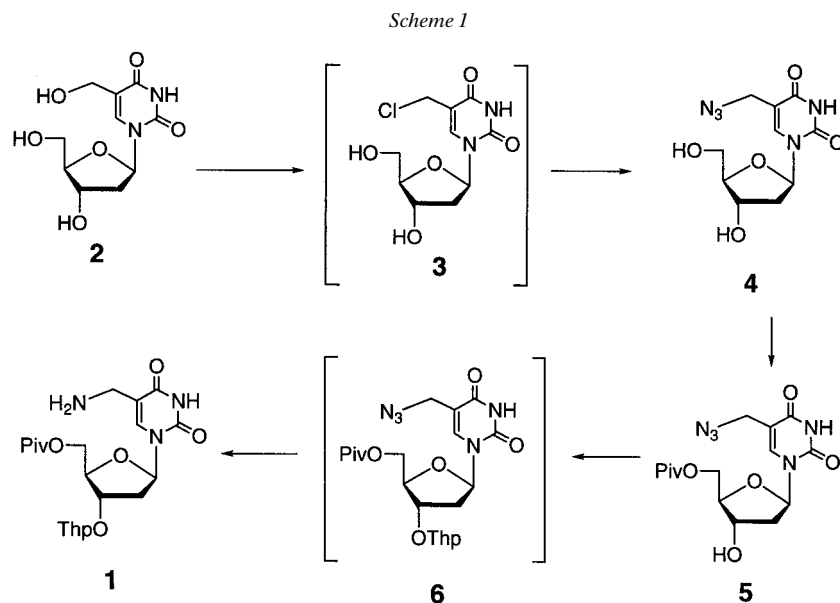
These bent DNAs or RNAs can apparently be stabilized by binding to proteins or their 3-dimensional structures. If such a bent structure could be created independently from these complex interactions, a variety of intrinsic studies would be developed taking advantage of its inherent properties that cannot be acquired from the usual linear DNAs or RNAs. For example, unique motifs, such as extremely stabilized loops or duplexes with a bulge-out or flip-out structure, could be generated.

Therefore, it is of great interest to create an artificially bent motif by introducing a chemically modified nucleotide unit having a rigid bent backbone structure into oligonucleotides. We previously reported our studies of chemical fixation of uridylic acid [4] and uridylyl-(3' → 5')-uridine [5] in conformations similar to those of a mononucleotide unit seen in the A-type RNA duplex and a sharply bent U-turn structure existing in the tRNA anticodon loop, respectively, by introducing covalent

bonding bridges into the parent structures. Preliminary molecular-mechanics calculation analysis of the cyclic uridylyl-(3' → 5')-uridine [5] having a CH₂C(O)NHCH₂ linker revealed a two-state equilibrium between the turn and stretch conformations. The NMR studies suggested that the latter is more stable than the former and has a bending property because of the fixed orientation of the two bases.

In this paper, we report the synthesis and conformational analysis of a uridylyl-(3' → 5')-2'-deoxyuridine derivative having the covalent-bonding linker and the synthesis of oligothymidylates containing this cyclic dimer. Conformation of the dimer unit and the modified oligothymidylates was analyzed by spectroscopic, electrophoretic, and computational methods.

2. Results and Discussion. – 2.1. *Chemical Synthesis of the 3'-Terminal Nucleoside Unit 1.* The 3'-terminal nucleoside unit **1** was synthesized from 5-(hydroxymethyl)-2'-deoxyuridine (**2**) [6] by treatment with chlorotrimethylsilane in dioxane [7] (→ **3**) and then with sodium azide in DMF *via* 5-(azidomethyl)-2'-deoxyuridine (**4**; 73% yield) (*Scheme 1*). The reaction of **4** with pivaloyl chloride (pivCl) in pyridine gave the selectively 5'-protected product **5** in 70% yield. The 3'-tetrahydropyranylation (Thp) of **5** (→ **6**) followed by Pd/C-catalyzed hydrogenation furnished the 3'-terminal nucleoside unit **1** in an overall yield of 64% from **5**.



2.2. *Chemical Synthesis of the Interresidually Cyclized Uridylyl-(3' → 5')-2'-deoxyuridine 14.* The interresidually cyclized uridylyl-(3' → 5')-2'-deoxyuridine **14** was synthesized from the 3'-terminal nucleoside unit **1** and the 5'-terminal nucleoside unit **7** [7] (*Scheme 2*). First, acid **7** was converted to ester **8** by treatment with *N*-

hydroxysuccinimide in the presence of *N*-[3-(dimethylamino)propyl] *N'*-ethyl-carbodiimide hydrochloride (EDC) [8]. Condensation of the activated ester **8** with **1** in the presence of Et₃N gave the protected dimer **9** in 86% yield. The *t*-BuMe₂Si group of **9** was removed by treatment with tetrabutylammonium fluoride hydrate to give alcohol **10** in 71% yield, and the liberated 3'-hydroxy group of the 5'-upstream nucleoside was phosphorylated by treatment with cyclohexylammonium *S,S'*-diphenyl phosphorodithioate [9] in the presence of isodurenedisulfonyl dichloride (DDS) [9] and 1*H*-tetrazole [10] to give the phosphorodithioate derivative **11** in 76% yield. The conversion of **11** to the cyclized dimer **13** was accomplished in 64% yield by the intramolecular *in situ* cyclization of the phosphotriester intermediate **12**, which was obtained by alkaline hydrolysis of **11**, under the conditions using DDS as a condensing reagent and 1*H*-tetrazole as a nucleophilic catalyst. The successive deprotection of the cyclized dimer **13** by treatment with aqueous KOH solution and then with 80% AcOH gave the cyclized uridylyl-(3' → 5')-2'-deoxyuridine derivative **14** in 58% yield (*Scheme 2*). The detailed conformation of the fully deprotected cyclic dimer **14** is described in *Sect. 2.3*, and the results were used in *Sect. 2.5* to predict the 3D structure of the oligonucleotide containing the dimer unit **14**.

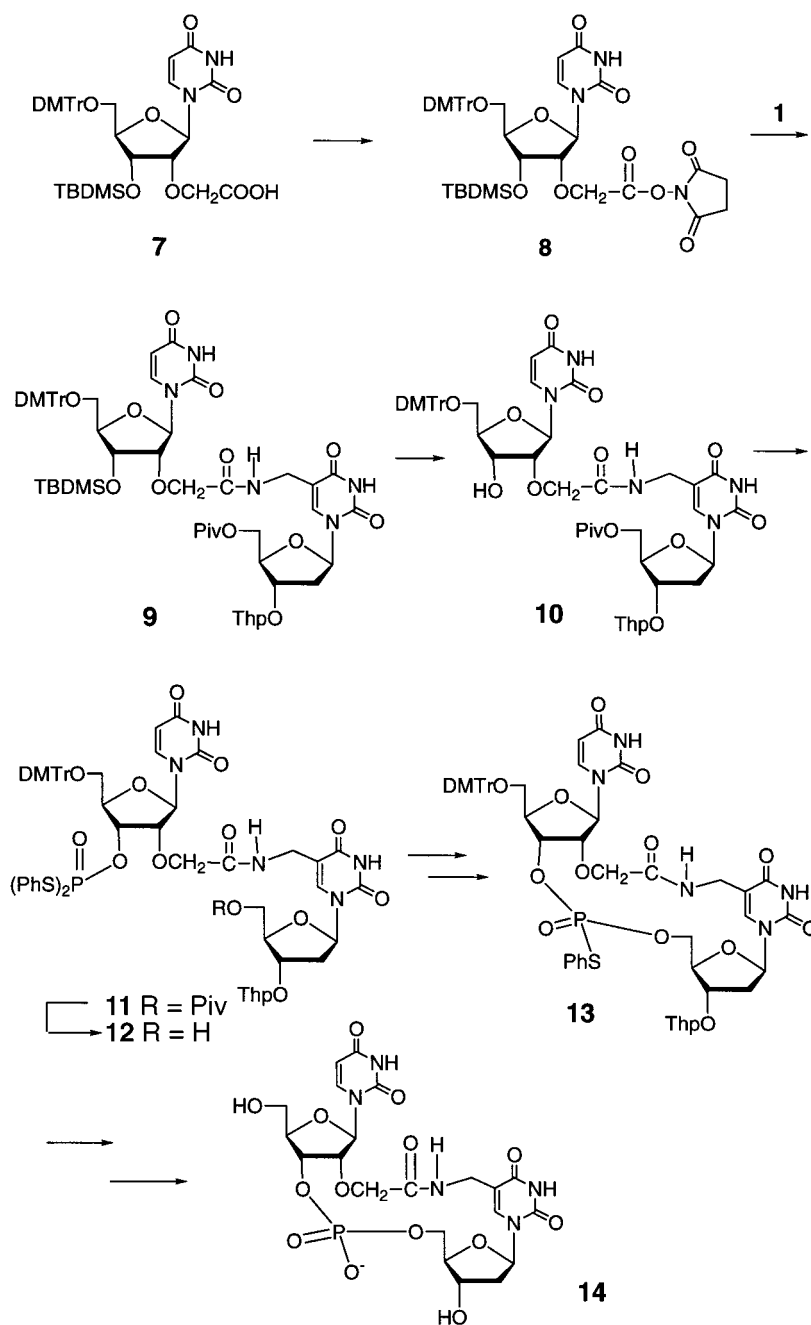
To incorporate the cyclized dimer unit into an oligonucleotide, the phosphoramidite unit **17** of the cyclized dimer was synthesized *via* **13** as a synthetic intermediate (*Scheme 3*). The (MeO)₂Tr and Thp groups of **13** were removed under acidic conditions (→ **15**), and the free 5'-hydroxy group of the 5'-upstream nucleoside unit was protected again with the (MeO)₂Tr group to give the 3'-hydroxy derivative **16** in 78% yield. The latter was then phosphitylated by treatment with 1.2 equiv. of 2-cyanoethyl diisopropylphosphoramidochloridite (=chloro(diisopropylamino)(2-cyanoethoxy)phosphine) [11] in the presence of 1.2 equiv. of ethyldiisopropylamine as a base to give the desired phosphoramidite unit **17** in 71% yield.

The ³¹P-NMR spectrum of **17** showed four signals near 150 ppm (146.99, 150.10, 150.35, and 150.44 ppm), which are derived from the phosphoramidite groups of the four diastereoisomers, and three signals around 25 ppm (24.78, 24.86, and 25.01 ppm) with the intensity ratio of 1:2:1, which are ascribed to the internucleotidic phosphoryl groups attached to the S-atom.

2.3. Conformational Analysis of the Cyclized Uridylyl-(3' → 5')-2'-deoxyuridine **14**.

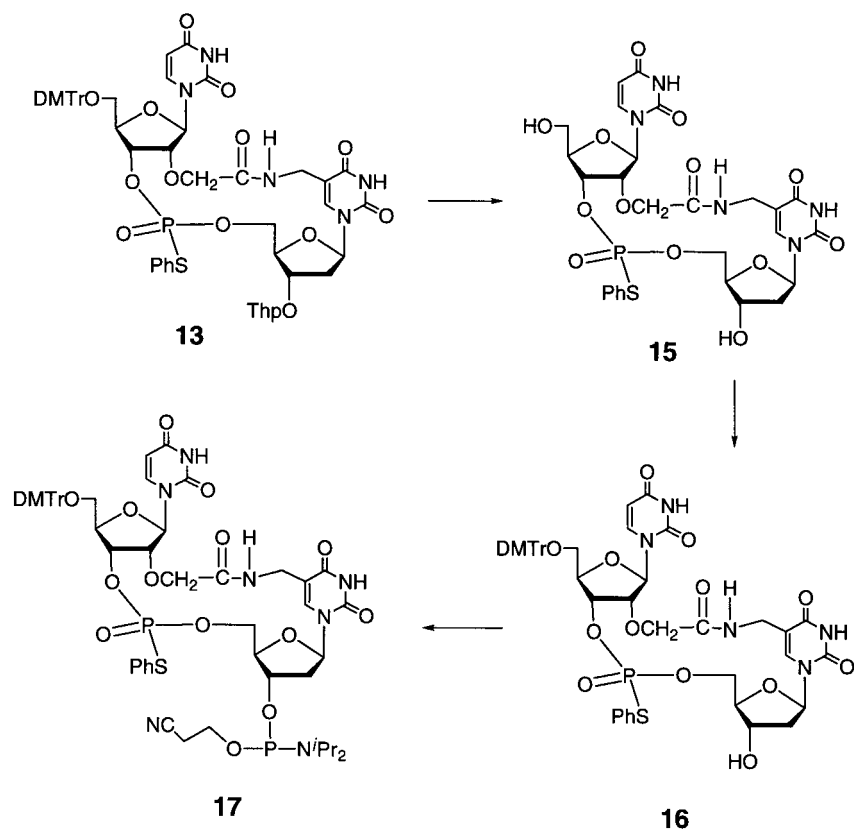
2.3.1. *Circular Dichroism (CD) Studies.* The CD spectra of cUpdU (**14**) and unmodified uridylyl-(3' → 5')-uridine (UpU) at 20 and 80° are shown in *Fig. 1*. The *Cotton* effect around 270 nm is the most important for the analysis of the conformational properties of these dinucleoside monophosphates because the CD pattern in this region reflects the orientation and interaction of the pyrimidine base of the 3'- and 5'-terminal nucleoside unit [12]. In the CD spectra of UpU, the intensity of this *Cotton* effect at 80° decreased to 60% at 20° indicating the conformational flexibility of UpU. In contrast, the intensity of the *Cotton* effect of cUpdU at 80° was maintained at 80% at 20°. This different temperature dependence clearly pointed to an increased conformational rigidity of cUpdU (**14**) induced by the cyclic structure. In the previous study of similarly cyclized dimers, in which the 3'-terminal nucleoside of **14** was replaced by a ribonucleoside, a similar conformational rigidity was observed in the CD spectra; the conformation was more rigid in the 3'-downstream ribonucleoside derivative than in **14** [5]. In general, the conformations of ribonucleosides are more rigid than those of

Scheme 2



DMTr = (MeO)₂Tr, TBDMS = ^tBuMe₂Si, Piv = Me₃CCO, Thp = tetrahydro-2H-pyran-2-yl.

Scheme 3



DMTr = (MeO)₂Tr, Thp = tetrahydro-2*H*-pyran-2-yl

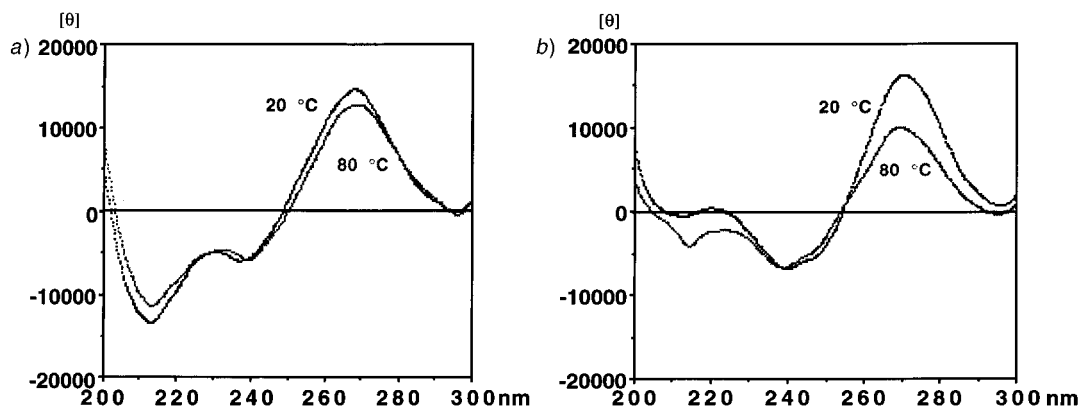


Fig. 1. CD Spectra of a) cUpdU (14) and b) UpU. In 10 mM sodium phosphate (pH 7.0) at 20 and 80°.

deoxyribonucleosides because of the additional electronic and steric effect of the 2'-hydroxy group [13]. This is also true for the cyclic dimers. The conformational rigidity of cUpdU is a suitable property for the stabilization of bent structures by incorporating this cyclized dimer unit into an oligonucleotide.

2.3.2. *Analysis of the Ribose Conformation by ¹H-NMR.* The ribose moiety of the natural nucleic acids is in equilibrium between the *N*-type and *S*-type conformers [14] (Fig. 2). Therefore, the conformation of the ribose moiety is described by the respective population of the *N*-type conformation ($P(N\text{-type})$) and the *S*-type conformation ($P(S\text{-type})$). The population of each conformer is calculated from the H,H-coupling constants between the protons on the ribose or deoxyribose ring.

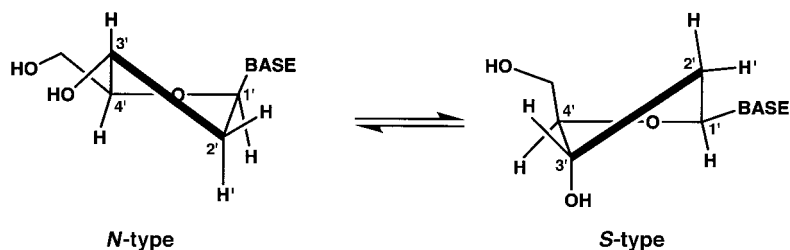


Fig. 2. The two major conformers of deoxyribonucleosides which exist in equilibrium

The H,H- and H,P-coupling constants of **14**, measured at 400 MHz, are shown in Table 1. Among the H,H-coupling constants of the ribose moiety, the $J(2',3')$ and $J(1',2') + J(3',4')$ values are of special importance. These values are nearly constant in natural or synthetic ribonucleic-acid derivatives having no structural constraints; the average values of $J(2',3')$ and $J(1',2') + J(3',4')$ are 5.2 Hz and 9.8 Hz, respectively [15]. Structurally constrained nucleic acids have values deviated from these typical ones. From this point of view, the rather smaller $J(1',2') + J(3',4')$ (7.4 Hz) of the 5'-upstream ribose of cUpdU indicates some distortion of the ribose conformation. However, the distortion might be small, because the Karplus equation [16] suggested that the $J(2',3')$ value of 5 Hz is realized only when the two equilibrium conformations are *N*-type and *S*-type regardless of the puckering amplitude (Fig. 3) and the $J(2',3')$ value of the cyclized dimer (4.8 Hz) is close to 5 Hz. Hence, the smaller $J(1',2') + J(3',4')$ observed would be explained by the *S*-type and *N*-type conformers with small distortion. In contrast, the conformation of the 3'-downstream deoxyribose moiety of **14** is not distorted because both the $J(2',3')$ (6.1 Hz) and $J(1',2') + J(3',4')$ (10.2 Hz) are close to the standard values observed for the natural 2'-deoxyribonucleosides (6.6 and 10.5 Hz, resp.). The $P(N\text{-type})$ and $P(S\text{-type})$ of both the 5'-upstream and 3'-downstream sugar moieties were calculated with the formula $P(N\text{-type}) = J(3',4') / (J(1',2') + J(3',4'))$ [16]. Consequently, the $P(N\text{-type})$ of the 5'-upstream ribose residue is 38%, while the $P(N\text{-type})$ of the 3'-downstream deoxyribose residue is 33%. In brief, the major conformers of both the 5'- and 3'-terminal sugars are *S*-type. The population $P(S\text{-type})$ is 60–70%.

2.3.3. *NOESY Spectrum of cUpdU.* To obtain information on the relative location of the 5'-upstream and 3'-downstream residues, the NOESY spectrum of cUpdU was

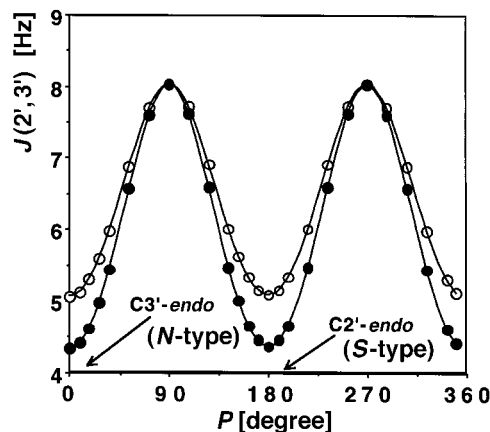


Fig. 3. Simulation of $J(2',3')$ by the Karplus equation [16]. P = phase angle of pseudorotation. Plots of the values obtained from the simulations with the puckering amplitude fixed at 35° (\circ) and 40° (\bullet).

Table 1. H,H Coupling Constants [Hz] in the 1H -NMR Spectrum (400 MHz) of **14**^a

| | Coupling constant J [Hz] | | | | | | |
|------------------------|----------------------------|-------------|------------|-------------|------------|------------|-------------|
| | $J(1',2')$ | $J(1',2'')$ | $J(2',3')$ | $J(2'',3')$ | $J(3',4')$ | $J(4',5')$ | $J(4',5'')$ |
| 5'-Terminal nucleoside | 4.6 | – | 4.8 | – | 2.8 | 2.8 | 4.0 |
| 3'-Terminal nucleoside | 6.7 | 6.7 | 3.7 | 6.1 | 3.5 | n.d. | n.d. |

^a) The critical values for the determination of the ribose or deoxyribose conformation are written in italics.

^b) Measured at 109 MHz.

recorded. Although many cross-peaks are present, all of them are derived from the intraresidual H,H interactions, and no interresidual cross-peaks are observed. This result indicates that cUpdU has a conformation in which the distance between the 5'- and 3'-terminal nucleoside units is long. This distance information based on the interresidual H,H interactions was used to analyze the molecular-mechanics simulation results of the 3D structure of **14** described in Sect. 2.3.4.

2.3.4. Molecular-Mechanics Studies. Detailed three-dimensional model structures of the cyclic dimer **14** were built by molecular-mechanics calculations with the MonteCarlo conformation search and energy minimization [17]. The AMBER* force field [18][19] and GB/SA solvent model [19] were used in all simulations. Four calculation runs were carried out, in which the ribose moieties of the 5'-upstream and 3'-downstream nucleoside units were fixed in the {*N*-type and *N*-type} (**A**), {*N*-type and *S*-type} (**B**), {*S*-type and *N*-type} (**C**), and {*S*-type and *S*-type} (**D**) conformations, respectively. The ribose moieties were fixed in the standard *N*- and *S*-type conformations because the AMBER* force field did not give results compatible with the experimental data in terms of ribose conformation in our test simulations (data not shown). The structures having the lowest energies obtained from each run are shown in Fig. 4.

The structures **A** – **C** can be divided into two categories, namely, the 'turn' (**A** and **B** in Fig. 4) and 'bent' forms (**C** and **D**). The two runs in which the ribose moiety of the 5'-

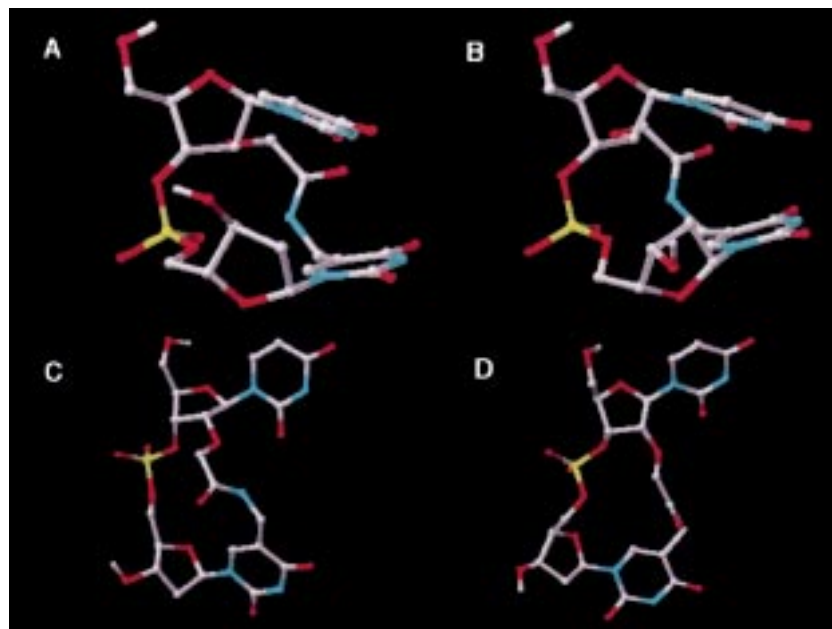


Fig. 4. Low-energy structures of *cUpdU* (**14**) calculated by fixing the 5'-terminal ribose and 3'-terminal deoxyribose moieties in the [N-type and N-type] (**A**), [N-type and S-type] (**B**), [S-type and N-type] (**C**), and [S-type and S-type] (**D**) conformation

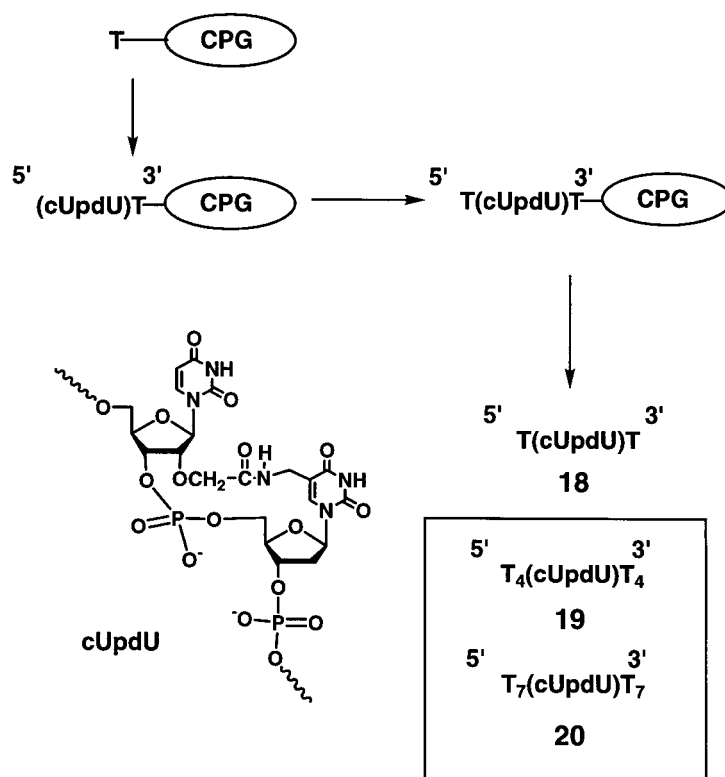
upstream nucleoside unit was fixed in the *N*-type conformation gave energetically unfavorable turn conformations ($E = -882.74$ and -888.68 kJ/mol for **A** and **B**, resp.), whereas the two runs in which the ribose moiety of the 5'-upstream nucleoside units was fixed in the *S*-type conformation gave energetically more favorable bent conformers ($E = -893.02$ and -893.03 kJ/mol for **C** and **D**, resp.). In the turn conformers, the distance between the 5'-upstream and 3'-downstream residues is short enough to allow NOEs between the interresidual protons. For example, the inter-proton distances H–C(2')(5'-upstream residue)/H–C(3')(3'-downstream residue), H–C(2')(5'-upstream residue)/H–C(2')(3'-downstream residue), H–C(3')(5'-upstream residue)/H–C(3')(3'-downstream residue), and H–C(3')(5'-upstream residue)/H–C(2')(3'-downstream residue) are 4.78, 2.80, 3.18, and 2.37 Å, respectively, for conformer **A**, and 2.66, 4.42, 2.31, and 4.64 Å, respectively, for conformer **B**. In the bent conformers **C** and **D**, the interresidual distances are too long to give NOEs. Thus, the structural properties of the bent conformers are in agreement with the properties of **14** established by the H,H coupling constants (Sect. 2.3.2) and NOESY spectrum (Sect. 2.3.3), *i.e.*, the major conformer of the cyclic dimer has an *S*-type ribose at the 5'-terminus, with a long distance between the 5'- and 3'-terminal residues. Therefore, the three-dimensional structure of **14** in aqueous solution must be similar to that shown for **C** and **D** (Fig. 4).

From the above conformation analyses by means of CD and $^1\text{H-NMR}$ spectroscopy and molecular mechanics, it was concluded that the cyclic dimer **14** has a rigid conformation with the *S*-type ribose conformation and long interresidual distance. Thus, the dinucleoside monophosphate **14** having these conformational properties is

highly recommendable as the dimer unit to be introduced into the oligonucleotides as a rigid bent structure.

2.4. *Chemical Synthesis of the Oligonucleotide Having a Bent Structure.* An oligothymidylate having a bent structure was synthesized by using the phosphoramidite dimer unit **17**, derived from **14**. First, the tetrathymidylate **18** was synthesized to confirm the efficient introduction of the dimer unit under the standard conditions used in the solid-phase synthesis (*Scheme 4*). The coupling reaction, according to the general solid-phase oligonucleotide synthesis, followed by the treatments with aqueous NaOH solution and then with 80% AcOH, gave the tetramer **18**. The structure of **18** was supported by the ^1H - and ^{31}P -NMR spectra (D_2O); a low-field $\delta(\text{P})$ indicating that the bent structure stabilized by the cyclic amide linkage was preserved even in the oligonucleotide because the low-field shift of the internucleotidic phosphate is the general indicator of the bent backbone conformation [20].

Scheme 4



The ^1H -NMR spectra of tetramer **18** in D_2O showed the signals of the Me groups of the two thymine bases around 1.9 ppm and four signals of the 6 protons of the four pyrimidine bases around 7.5–7.9 ppm. The ^{31}P -NMR spectra gave three signals due to the three internucleotidic phosphate groups around 0 ppm. The $\delta(\text{P})$ of the internucleotidic phosphate of the cyclic dimer unit was found in the lowest field in the ^{31}P -NMR spectrum.

2.5. Conformational Properties of the Decanucleotide Having a Cyclic Dimer Unit.

A decathymidylate **19** having the cyclic-dimer unit **14** at the center was synthesized by the solid-phase synthesis. The decathymidylate **19** was expected to have a bent structure induced by the cyclic structure.

It is well known that a change in three-dimensional DNA duplex structures is reflected sensitively by the mobility in polyacrylamide-gel electrophoresis (PAGE) [21]. The 20% PAGE of the decathymidylate **19**, T_{10} , and T_{11} are shown in Fig. 5. The molecular-mass difference between **19** and T_{10} ($\Delta M_r = 57$) is smaller than that between **19** and T_{11} ($\Delta M_r = 246$). On the contrary, the difference in the gel shift between **19** and T_{10} is larger than that between **19** and T_{11} . This result indicates a rigid structure for **19**, which is induced by introduction of the cyclic dimer unit **14**, thereby restraining the mobility of **19** on PAGE.



Fig. 5. 20% PAGE of $T_4(cUpdU)T_4$ (**19**), T_{11} , and T_{10} . Lanes 1 and 5, bromophenol blue; Lane 2, T_{11} ; Lane 3, **19**; Lane 4, T_{10} .

The rigid conformation of **19** was also reflected in a smaller temperature dependence of its CD spectra at 20, 40, and 80° compared to those of T_{10} at these temperatures (Fig. 6, a and b, resp.). Although the cyclic structure unit of **19** reduces the conformational flexibility, it seems only effective near the modified site and is not likely to affect the overall conformation of the oligomer because the whole shape of the CD spectra of **19** is similar to that of T_{10} . Oligomer **19** having a locally fixed conformation as described above, would be suitable for the modification of a duplex structure when hybridized to its complementary strand (see Sect. 2.6).

2.6. Duplex Formation of the Deca- or Hexadecathymidylates Having a Cyclic Dimer Unit. The decathymidylate **19** was mixed with an equimolar amount of dA_{10} , and the UV melting curve of the duplex formed was recorded and compared with that of $T_{10} \cdot dA_{10}$ (Fig. 7 and Table 2). The considerable decrease of the T_m value of **19** · dA_{10} compared with that of $T_{10} \cdot dA_{10}$ ($\Delta T_m = -20^\circ$) suggested disruption of base pairing.

The model structure of the disrupted base pairing and the whole duplex was built by replacing the fifth and sixth thymidine units of T_{10} by the turn (Fig. 4, B) or bent

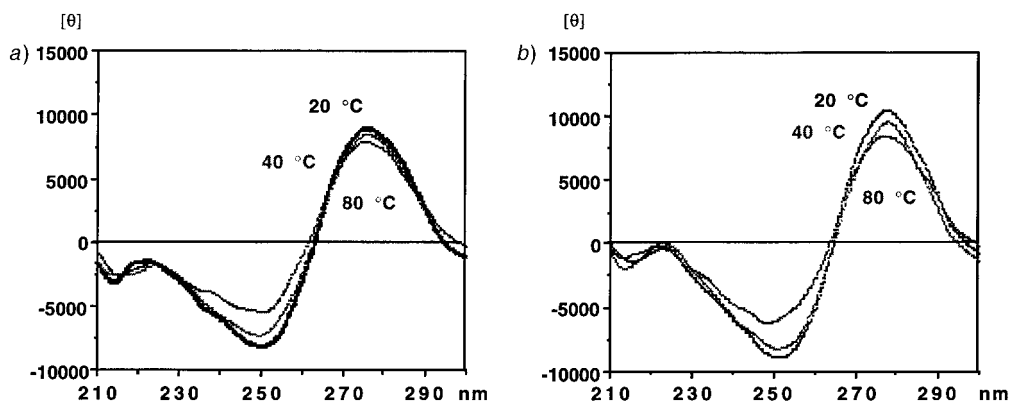


Fig. 6. CD Spectra a) of decathymidylate **19** containing the cyclic dimer unit and b) of decathymidylate T_{10} . In 10 mM sodium phosphate (pH 7.0).

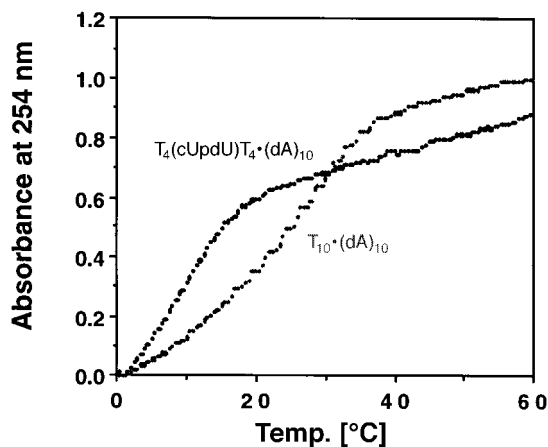


Fig. 7. UV Melting curves of the duplexes $T_4(\text{cUpdU})T_4 \cdot (\text{dA})_{10}$ and of decathymidylate \cdot decadeoxyadenosine ($T_{10} \cdot (\text{dA})_{10}$). Measured in 10 mM sodium phosphate and 150 mM NaCl (pH 7.0)

Table 2. Melting Temperature [$^{\circ}$] of the DNA Duplexes $\mathbf{19} \cdot \text{dA}_{10}$, $T_{10} \cdot \text{dA}_{10}$, and $\mathbf{20} \cdot \text{dA}_n$ ($n = 14 - 19$). Measured in 10 mM sodium phosphate – 150 mM NaCl buffer

| | $\mathbf{19} \cdot (\text{dA})_{10}$ | $T_{10} \cdot (\text{dA})_{10}$ | $\mathbf{20} \cdot (\text{dA})_{14}$ | $\mathbf{20} \cdot (\text{dA})_{15}$ | $\mathbf{20} \cdot (\text{dA})_{16}$ | $\mathbf{20} \cdot (\text{dA})_{17}$ | $\mathbf{20} \cdot (\text{dA})_{18}$ | $\mathbf{20} \cdot (\text{dA})_{19}$ |
|----------------------|--------------------------------------|---------------------------------|--------------------------------------|--------------------------------------|--------------------------------------|--------------------------------------|--------------------------------------|--------------------------------------|
| T_m [$^{\circ}$] | 8 | 28 | 26.5 | 30.3 | 32.0 | 33.0 | 33.2 | 33.0 |

conformer of **14** (Fig. 4, **D**) on the computer graphics (Fig. 8). While the decathymidylate containing the turn conformer **B** (see Fig. 8, **E**) does not seem suitable for duplex formation because of its extremely sharp bend, the one containing the bent conformer **D** (see Fig. 8, **F**) seems suitable. However, the distance between the N(1)-atoms on the 5'- and 3'-terminal pyrimidine rings of the cyclic dimer unit is *ca.* 9 Å, which is twice as long as the distance seen in the standard B-type duplex (4 Å) [22]. Therefore, the disruption of the base pairing could occur at this site.

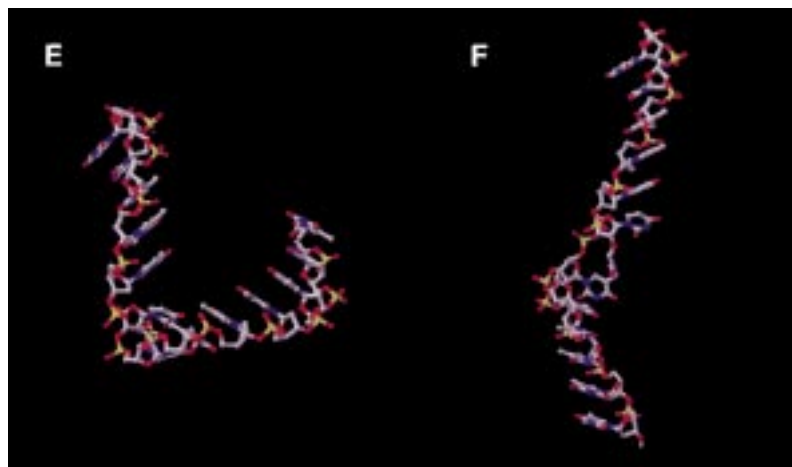


Fig. 8. Predicted structures **E** and **F** of a dodecathymidylate $T_5(cUpdU)T_5$ incorporating the turn conformer **B** and the bent conformer **D**, respectively, of Fig. 4

There are two plausible models for the disrupted duplex structure. One is the ‘bulge-out’ structure in which a single deoxyadenosine residue at the site opposite to the cyclic dimer unit bulges out to compensate for the widened internucleotidic distance in the oligothymidylate strand, and the other is the ‘no-bulge-out’ structure in which no adenosine residue bulges out but the base-pairing is distorted because of the unusual geometry. If the ‘bulge-out’ model structure is correct, either the 5'- or 3'-terminal deoxythymidine residue must dangle without forming any base-pairing when the lengths of the oligothymidylates containing a cyclic-dimer unit and the oligodeoxyadenylate are the same. Therefore, the validity of this model must be examined by measuring the dependence of the T_m values on the chain length of the oligodeoxyadenylate.

Because the T_m values of the oligodeoxyadenylate·**19** duplexes were too low to give correct T_m values when the chain length of the oligodeoxyadenylate was altered, the hexadecathymidylate **20** was synthesized, and the T_m values of the duplex formation between **20** and oligodeoxyadenylates (dA)₁₄ to (dA)₁₉ having the chain length of 14–19 units were measured (Fig. 9 and Table 2). The T_m values of the duplexes formed between **20** and oligodeoxyadenylates (dA)₁₄ to (dA)₁₉ rose with the length of the oligodeoxyadenylate increasing from 14 to 17 units, and then reached a plateau (Fig. 10). These observations are consistent with the ‘bulge-out’ model described above wherein the terminal residues of the oligothymidylate strand dangle until the oligodeoxyadenylate chain is lengthened up to (dA)₁₆, but the number of base-pairing is constant after the chain length has reached 17 units. Shown in Fig. 11 is the duplex model structure of **20**·(dA)₁₇ which has the bulged-out adenosine residue at the middle of the duplex. In this model, the duplex bends by *ca.* 30°, and the base-pairings are loosened at the middle of the strand. This base-pair disruption could contribute to the observed duplex instability.

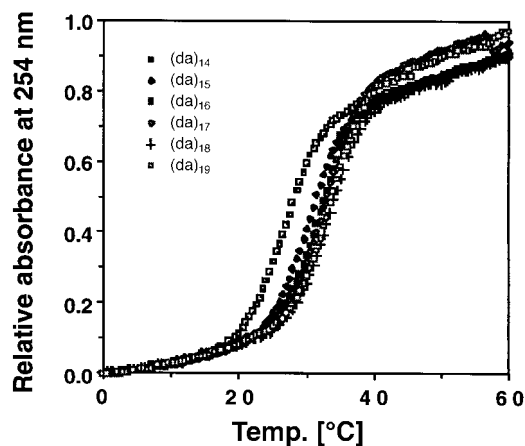


Fig. 9. UV Melting curves of the duplexes $T_7(cUpdU)T_7 \cdot \text{oligodeoxyadenylate } (20 \cdot (\text{dA})_n)$ having various chain lengths. Measured in 10 mM sodium phosphate and 150 mM NaCl (pH 7.0). The vertical axis indicates the relative absorbance when the absorbance at 90° is normalized to unity.

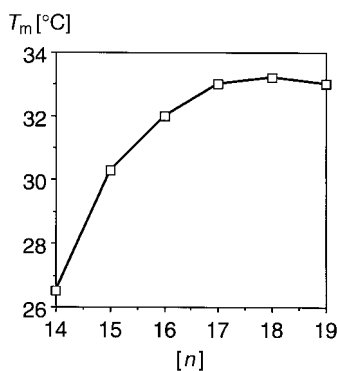


Fig. 10. Relationship between the number n of nucleotide units in the oligodeoxyadenylate chain and the T_m values [°] of the duplexes $T_7(cUpdU)T_7 \cdot \text{oligodeoxyadenylate } (20 \cdot (\text{dA})_n)$ having various chain lengths (see Table 2)

3. Conclusions. – In this study, an artificially bent DNA strand was chemically synthesized for the first time by the introduction of a conformationally rigid cyclized UpdU dimer at the center of oligothymidylates. No other report on the synthesis of such bent DNA oligomers by chemical approaches has been published to date. Since an increasing number of studies on DNA-protein and RNA-protein interactions [2] have revealed that DNA bending is a crucial step in the regulation of the function of nucleic acids [1], it is of great importance to have available an artificially bent structure of DNA or RNA that will be useful as a fixed bent motif for investigating the structure-function relationship of bent DNA or RNA.

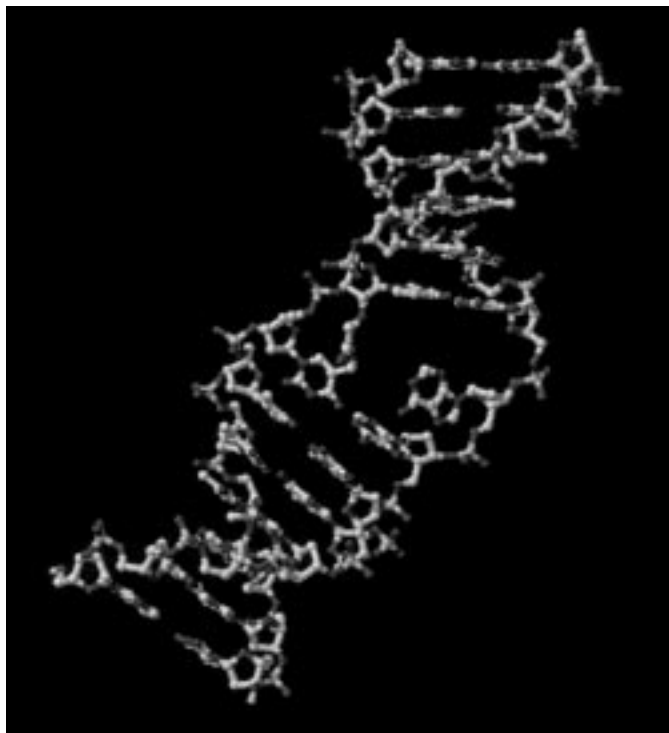


Fig. 11. Duplex model structure of $T_7(cUpdU)T_7 \cdot (dA)_{17}(\mathbf{20} \cdot (dA)_{17})$ which has a bulged-out adenosine residue at the middle of the duplex

Experimental Part

General. Pyridine was distilled twice from $TsCl$ and from CaH_2 and then stored over 4 \AA molecular sieves. TLC: Merck silica gel 60-F-254 (0.25 mm). Column chromatography (CC): silica gel C-200 from Wako Co. Ltd.; a minipump for a goldfish bowl was conveniently used to attain sufficient pressure for rapid CC separation; reversed-phase CC with $\mu Bondapak-C-18$ silica gel (prep S-500, Waters). Reversed-phase HPLC: $\mu Bondasphere C-18$ column, linear gradient starting from 0.1M NH_4OAc (pH 7.0) and applying 0–30% of MeCN at a flow rate of 1.0 ml/min for 30 min. UV Spectra: Hitachi-U-2000 spectrometer; λ_{max} in nm. CD Spectra: Jasco-J-500-C spectrometer, 0.5-cm cell. 1H -, ^{13}C -, and ^{31}P -NMR Spectra: at 270, 68, and 109 MHz, resp.; Jeol-EX270 spectrometer; chemical shifts δ in ppm rel. to $SiMe_4$ or DSS (sodium 3-(trimethylsilyl)propane-1-sulfonate) for 1H -NMR, $CDCl_3$ (= 77 ppm) or DSS (= 0 ppm) for ^{13}C -NMR, and 85% phosphoric acid (= 0 ppm) for ^{31}P -NMR, J in Hz; $J(H,H)$ and NOESY at 400 MHz with Varian-Unity-400 spectrometer; protons at the 5'-terminal unit are labelled with 'a', those at the 3'-terminal unit with 'b'. Elemental analyses were performed by the Microanalytical Laboratory, Tokyo Institute of Technology at Nagatsuta.

5-(Azidomethyl)-2'-deoxyuridine (4) [6]. To a soln. of 5-(hydroxymethyl)-2'-deoxyuridine [6] (9.0 g, 34.9 mmol) in 1,4-dioxane (250 ml) in a sealed tube, chlorotrimethylsilane (19.0 g, 175 mmol) was added. The soln. was stirred at 50° for 2.5 h and then evaporated, and the residue was dissolved in DMF (100 ml). NaN_3 (6.81 g, 105 mmol) was added, and the resulting soln. was stirred at 60° for 15 min. The precipitate was removed by filtration, the filtrate evaporated, and the residue submitted to CC (silica gel, $CH_2Cl_2/MeOH$ 100:5): **4** (7.5 g, 77%). M.p. $134-136^\circ$ ([6a] $133-135^\circ$). 1H - and ^{13}C -NMR: identical with those of the authentic sample [6b].

5-(Azidomethyl)-2'-deoxy-5'-O-pivaloyluridine (5). To a soln. of **4** (200 mg, 0.69 mmol) in pyridine (5 ml), pivaloyl chloride (111 μ l, 0.90 mmol) was added, and the resulting mixture was stirred for 1.5 h at r.t. The soln. was diluted with $CHCl_3$ (50 ml), washed with sat. aq. $NaHCO_3$ soln., dried (Na_2SO_4), and evaporated and the residue submitted to CC (silica gel, $CHCl_3/MeOH$ 100:2): **5** (177 mg, 70%). M.p. $153-154^\circ$ (hexane/AcOEt).

¹H-NMR (270 MHz, CDCl₃): 1.23 (s, 3 Me); 2.12 (m, H–C(2')); 2.50 (m, H–C(2)); 4.09–4.45 (m, H–C(3'), H–C(5'), CH₂N₃); 4.48 (m, H–C(4'), H–C(5)); 6.23 (m, H–C(1')); 7.52 (s, H–C(6)); 8.40 (br., NH). ¹³C-NMR (68 MHz, CDCl₃): 27.17; 38.89; 40.74; 47.10; 63.65; 71.52; 84.75; 85.59; 109.92; 137.70. Anal. calc. for C₁₅H₂₁N₃O₆: C 49.05, H 5.76, N 19.06; found: C 49.17, H 5.86, N 18.83.

5-(Aminomethyl)-2'-deoxy-5'-O-pivaloyl-3'-O-(tetrahydro-2H-pyran-2-yl)uridine (**1**). To a soln. of **5** (5.4 g, 14.7 mmol) in CH₂Cl₂ (150 ml) 1,4-dihydro-2H-pyran (27 ml, 294 mmol) and CF₃COOH (570 μl, 7.4 mmol) were added, and the resulting mixture was stirred for 10 h. The mixture was washed with sat. aq. NaHCO₃ soln., the org. layer dried (Na₂SO₄) and evaporated, and the residue dissolved in MeOH (150 ml). To this soln., Pd/C (1 g) was added, and the mixture was stirred for 14 h under H₂. Pd/C was removed by filtration, the filtrate evaporated and the residue submitted to CC (silica gel, CHCl₃/MeOH 100:2): **1** (4.0 g, 64%). ¹H-NMR (270 MHz, CDCl₃): 1.18 (m, 3 Me); 1.82 (m, 3 CH₂); 2.05 (m, H'–C(2')); 2.48 (m, H–C(2')); 3.60 (s, CH₂N); 3.80 (m, CH₂O); 4.18–4.40 (m, H–C(3'), H–C(4'), 2 H–C(5')); 4.67 (s, OCHO); 6.25 (m, H–C(1')); 7.45, 7.42 (2s, H–C(6)). ¹³C-NMR (68 MHz, CDCl₃): 19.21; 19.27; 25.21; 27.21; 30.55; 30.60; 37.77; 38.74; 38.83; 39.46; 62.68; 63.79; 63.90; 75.35; 76.14; 82.27; 83.04; 85.18; 85.50; 97.86; 98.40; 116.14; 135.33; 135.45; 150.01; 163.09; 178.11. Anal. calc. for C₂₀H₃₁N₃O₇·1/2 H₂O: C 55.35, H 7.34, N 9.67; found: C 55.31, H 7.56, N 8.65.

3'-O-[(tert-Butyl)dimethylsilyl]-2'-O-[2-[[[1-2'-deoxy-5'-O-pivaloyl-3'-O-(tetrahydro-2H-pyran-2-yl)-β-D-ribofuranosyl]-1,2,3,4-tetrahydro-2,4-dioxypyrimidin-5-yl]methyl]amino]-2-oxoethyl]-5'-O-(4,4'-dimethoxytrityl)uridine (**9**). N-[3-(Dimethylamino)propyl]-N-ethylcarbodiimide hydrochloride (58 mg, 0.3 mmol) and N-hydroxysuccinimide (35 mg, 0.3 mmol) were added to a soln. of **7** (148 mg, 0.2 mmol) in DMF (2 ml). After 7.5 h, **1** (85 mg, 0.2 mmol) and Et₃N (28 μl, 0.2 mmol) were added, and the resulting soln. was stirred for 1 h. The mixture was partitioned between CHCl₃ and sat. aq. NaHCO₃ soln., and the org. layer was washed 5 times with sat. aq. NaHCO₃ soln., dried (Na₂CO₃), and evaporated. The residue was submitted to CC (silica gel, CHCl₃/MeOH 100:1): **9** (197 mg, 86%). ¹H-NMR (270 MHz, CDCl₃): –0.12, 0.12 (m, 2 MeSi); 0.72, 0.83 (2s, 6 and 3 H, 3 Me); 1.18 (s, 3 Me); 1.72 (m, 3 CH₂); 2.22 (m, H_b'–C(2')); 2.48 (m, H_b–C(2')); 3.31 (m, H_a'–C(5')); 3.50 (m, H_a–C(5')); 3.81 (m, 2 MeO, CH₂O); 4.02–4.40 (m, H_b–C(3'), H_b–C(4'), 2 H_b–C(5'), CH₂N, CH₂CO, H_a–C(4')); 4.68 (br., OCHO), 5.28 (d, J(5,6) = 7.9, H_a–C(5)); 5.94 (s, H_a–C(1')); 6.25 (m, H_b–C(1')); 6.82–6.87 (m, 4 arom. H); 7.21–7.35 (m, 9 arom. H); 7.58 (s, H_b–C(6)); 8.05 (d, J(5,6) = 7.9, H_a–C(6)); 9.05, 8.76 (2 br. m, each 1 H, NH(3)). ¹³C-NMR (68 MHz, CDCl₃): –5.23; –4.58; 17.70; 19.16; 25.11; 25.41; 27.10; 30.48; 35.67; 37.38; 38.35; 38.67; 55.11; 60.68; 62.43; 62.54; 63.67; 63.78; 69.53; 70.17; 75.38; 76.30; 82.14; 82.68; 82.80; 83.42; 85.21; 85.73; 86.97; 88.18; 97.66; 98.24; 102.21; 111.07; 113.10; 113.14; 127.15; 127.84; 128.23; 130.14; 134.79; 134.86; 138.35; 138.69; 139.43; 143.83; 150.10; 150.15; 150.48; 158.67; 163.54; 163.61; 169.27; 169.34; 177.95; 178.00. Anal. calc. for C₅₈H₇₅N₅O₁₆Si·H₂O: C 60.88, H 6.78, N 6.12; found: C 60.37, H 6.68, N 6.68.

2'-O-[2-[[[1-2'-Deoxy-5'-O-pivaloyl-3'-O-(tetrahydro-2H-pyran-2-yl)-β-D-ribofuranosyl]-1,2,3,4-tetrahydro-2,4-dioxypyrimidin-5-yl]methyl]amino]-2-oxoethyl]-5'-O-(4,4'-dimethoxytrityl)uridine (**10**). To a soln. of **9** (547 mg, 0.48 mmol) in THF (5 ml) tetrabutylammonium fluoride monohydrate (250 mg, 0.96 mmol) was added, and the soln. was stirred for 1 h. The mixture was diluted with CHCl₃ (50 ml), the soln. washed with H₂O (3 × 50 ml), dried (Na₂SO₄), and evaporated, and the residue submitted to CC (silica gel, CHCl₃/MeOH 100:2): **10** (354 mg, 71%). ¹H-NMR (270 MHz, CDCl₃): 1.21 (s, 3 Me); 1.46–1.87 (m, 3 CH₂); 2.05 (m, H_b'–C(2')); 2.50 (m, H_b–C(2')); 3.50 (m, 3 H, CH₂O, 2 H_a–C(5')); 3.68 (m, 7 H, CH₂O, 2 MeO); 4.02 (m, H_b–C(4')); 4.16–4.39 (m, H_a–C(2'), H_b–C(3'), H_a–C(4'), 2 H_b–C(5'), CH₂N, CH₂CO); 4.49 (m, H_a–C(3')); 4.68 (br., OCHO); 5.33 (d, J(5,6) = 8.2, H_a–C(5)); 5.84 (s, H_a–C(1')); 6.18 (m, H_b–C(1')); 6.82–6.88 (m, 4 arom. H); 7.22–7.41 (m, 9 arom. H); 7.67 (s, H_b–C(6)); 7.97 (d, J(5,6) = 7.9, H_a–C(6)); 10.24, 10.90 (2 br. m, each 1 H, NH(3)). ¹³C-NMR (68 MHz, CDCl₃): 19.14; 25.18; 27.21; 30.48; 36.10; 37.72; 38.80; 55.20; 61.42; 62.57; 63.65; 68.14; 69.62; 75.06; 76.17; 82.34; 83.09; 84.33; 85.43; 85.81; 86.85; 88.61; 97.75; 98.46; 102.35; 111.02; 113.12; 123.74; 127.03; 127.75; 127.92; 128.14; 129.11; 130.10; 130.17; 135.24; 135.44; 135.99; 139.10; 139.34; 139.46; 144.47; 149.70; 150.46; 151.32; 158.60; 163.23; 164.15; 170.39; 170.44; 178.17. Anal. calc. for C₅₂H₆₁N₅O₁₆·H₂O: C 60.64, H 6.16, N 6.79; found: C 60.52, H 6.12, N 6.29.

2'-O-[2-[[[1-2'-Deoxy-5'-O-pivaloyl-3'-O-(tetrahydro-2H-pyran-2-yl)-β-D-ribofuranosyl]-1,2,3,4-tetrahydro-2,4-dioxypyrimidin-5-yl]methyl]amino]-2-oxoethyl]-5'-O-(4,4'-dimethoxytrityl)uridine 3'-(S,S'-Diphenyl Phosphorodithioate) (**11**). Compound **10** (354 mg, 0.34 mmol) was rendered anhydrous by repeated co-evaporations with anh. pyridine and dissolved in anh. pyridine (5 ml). Cyclohexylammonium S,S'-diphenyl phosphorodithioate (191 mg, 0.68 mmol), isodurenedisulfonyl dichloride (= 2,4,5,6-tetramethylbenzene-1,3-disulfonyldichloride; 225 mg, 0.68 mmol), and 1H-tetrazole (95 mg, 1.36 mmol) were added, and the resulting soln. was stirred for 1 h. Then, the mixture was partitioned between CHCl₃ (20 ml) and sat. aq. NaHCO₃ soln. (20 ml). The org. phase was washed 5 times with sat. aq. NaHCO₃ soln., dried (Na₂SO₄), and evaporated and the residue co-evaporated repeatedly with toluene and then submitted to CC (silica gel, CHCl₃/MeOH 100:1): **11** (333 mg,

76%). ¹H-NMR (270 MHz, CDCl₃): 1.08 (s, 3 Me); 1.51–1.92 (m, 3 CH₂); 2.12 (m, H_b'-C(2')); 2.45 (m, H_b-C(2')); 3.38 (d, *J*_{gem} = 9.2, H_a'-C(5')); 3.48 (m, CH₂O, H_a-C(5')); 3.80 (m, 2 MeO, H_a-C(4')); 3.98–4.21 (m, H_a-C(2'), 2 H_b-C(5'), CH₂N, CH₂CO); 4.30 (m, H_b-C(3'), H_b-C(4')); 4.62 (br., OCHO); 5.12 (m, H_a-C(3')); 5.28 (d, *J*(5,6) = 7.8, H_a-C(5)); 6.08 (m, H_a-C(1')); 6.20 (m, H_b-C(1')); 6.82 (m, 4 arom. H); 7.20–7.58 (m, 19 arom. H); 7.70 (d, *J*(5,6) = 7.9, H_a-C(6)); 9.34, 9.55 (2br. m, each 1 H, NH(3)). ¹³C-NMR (68 MHz, CDCl₃): 19.21; 19.25; 25.20; 27.15; 27.21; 30.51; 35.76; 37.47; 38.46; 38.76; 55.20; 61.60; 62.52; 62.64; 63.76; 63.88; 70.32; 74.54; 75.44; 76.37; 82.00; 82.93; 85.36; 85.93; 86.49; 87.49; 97.74; 98.37; 102.91; 111.02; 111.05; 113.33; 125.25; 125.36; 125.75; 125.86; 127.30; 128.05; 128.14; 129.47; 129.51; 129.67; 129.72; 129.87; 129.92; 130.12; 134.65; 134.70; 135.08; 135.15; 135.51; 135.60; 138.63; 138.92; 139.05; 143.88; 149.98; 150.03; 158.78; 163.45; 163.49; 168.64; 168.73; 178.06; 178.09. ³¹P-NMR (109 MHz, CDCl₃): 52.09, 52.13. Anal. calc. for C₆₄H₇₀N₅O₁₇·2 H₂O: C 58.58, H 5.38, N 5.33; found: C 57.94, H 5.20, N 5.48.

{5'-2'-O-[Methyleneimino(2-oxoethane-2,1-diyl)]-Linked 5'-O-(4,4'-Dimethoxytrityl)-P-thiouridyl-(3' → 5')-2'-deoxy-3'-O-(tetrahydro-2H-pyran-2-yl)uridine S-Phenyl Ester (**13**). A soln. of **11** (750 mg, 0.58 mmol) in 0.5M KOH/pyridine 1:1 (40 ml) was stirred for 3 h. The soln. was neutralized with Dowex 50W × 8 (pyridinium salt, 2 × 5 cm). Et₃N (5 ml) was added and the solvent evaporated. The residue was rendered anhydrous by repeated co-evaporations (5 ×) with anh. pyridine and dissolved in anh. pyridine (30 ml). Isodurenedisulfonyl dichloride (384 mg, 1.16 mmol) and 1H-tetrazole (326 mg, 2.32 mmol) were added, and the mixture was stirred for 20 min. The mixture was diluted with CHCl₃ (100 ml), the soln. washed 3 times with sat. aq. NaHCO₃ soln., the org. phase dried (Na₂SO₄) and evaporated, and the residue submitted to CC (silica gel, CHCl₃/MeOH 100:1.5): **13** (444 mg, 65%). ¹H-NMR (270 MHz, CDCl₃): 1.38–1.82 (m, 3 CH₂); 2.05 (m, H_b'-C(2')); 2.52 (m, H_b-C(2')); 3.20 (m, H_a'-C(5')); 3.58 (m, CH₂O, H_a-C(5')); 3.80 (m, 2 MeO); 4.01–4.48 (m, H_a-C(2'), H_b-C(3'), H_b-C(4'), 2 H_b-C(5'), CH₂N, CH₂CO); 4.60 (br., H_a-C(4')); 4.61 (s, OCHO); 4.91 (m, H_a-C(3')); 5.31 (d, *J*(5,6) = 8.2, H_a-C(5)); 6.05 (m, H_a-C(1')); 6.21, 6.40 (2m, H_b-C(1')); 6.83–6.99 (m, 4 arom. H); 7.18–7.58 (m, 9 arom. H); 7.79 (m, H_a-C(6), H_b-C(6)); 9.02, 9.10, 9.38, 9.44 (NH(3)). ¹³C-NMR (68 MHz, CDCl₃): 19.01; 19.59; 25.18; 19.04; 29.63; 30.44; 30.64; 34.52; 38.19; 39.22; 55.22; 55.28; 62.18; 62.43; 62.61; 63.16; 68.20; 70.37; 75.29; 75.62; 75.81; 77.93; 81.38; 82.03; 82.16; 82.28; 82.43; 83.49; 85.57; 85.84; 86.02; 87.49; 87.78; 98.22; 98.40; 98.53; 102.93; 103.43; 111.52; 111.73; 112.20; 113.10; 113.32; 113.41; 124.22; 124.33; 124.44; 127.27; 127.48; 127.73; 128.12; 129.09; 129.74; 129.85; 134.14; 134.47; 134.56; 134.74; 134.91; 134.99; 138.85; 143.61; 143.90; 150.06; 150.21; 150.48; 150.57; 150.62; 158.78; 158.90; 162.17; 162.35; 162.41; 162.71; 163.04; 166.77; 168.30; 168.59. Anal. calc. for C₅₃H₅₆N₅O₁₆PS: C 58.83, H 5.22, N 6.47; found: C 58.53, H 5.78, N 6.57.

{5'-2'-O-[Methyleneimino(2-oxoethane-2,1-diyl)]-Linked Uridyl-(3' → 5')-2'-deoxyuridine (**14**). A soln. of **13** (77 mg, 65 μmol) in 0.2M NaOH/pyridine 1:1 (4 ml) was stirred for 5 min. The mixture was neutralized with Dowex 50W × 8 (pyridinium salt, 1 × 5 cm). The solvent was evaporated and the remaining pyridine was removed by repeated co-evaporations with H₂O. The residue was dissolved in 80% AcOH/H₂O and the soln. stirred for 20 h. The AcOH was removed by repeated co-evaporations with H₂O and the residue submitted to reversed-phase CC (C-18, H₂O/MeOH 100:8): **14** (760 A₂₆₀, 58%). The yield was estimated by assuming that ε₂₆₀ of **14** was identical with that of UpU (ε₂₆₀ 19600). ¹H-NMR (270 MHz, D₂O): 2.28 (ddd, *J*(1',2') = 6.7, *J*(2',3') = 3.7, *J*(2',2'') = 13.5, H_b'-C(2')); 2.46 (ddd, *J*(1',2'') = 6.7, *J*(2'',3') = 6.1, *J*(2',2'') = 13.5, H_b'-C(2'')); 3.90 (dd, *J*(5',5'') = 12.9, *J*(4',5'') = 4.0, H_a'-C(5'')); 3.98 (dd, *J*(5',5'') = 12.9, *J*(4',5') = 2.8, H_a-C(5'')); 4.18 (m, 2 H_b-C(5'')); 4.24 (m, H_b-C(4'), CH₂N); 4.38 (s, CH₂O); 4.40 (m, H_a-C(4')); 4.45 (dd, *J*(1',2') = 4.6, *J*(2',3') = 4.8, H_a-C(2'')); 4.55 (ddd, *J*(2',3') = 3.7, *J*(2'',3') = 6.1, *J*(3',4') = 3.5, H_b-C(3'')); 4.82 (ddd, *J*(2',3') = 4.8, *J*(3',4') = 2.8, *J*(3',P) = 8.0, H_a-C(3'')); 5.90 (d, *J*(5,6) = 8.0, H_a-C(5)); 6.13 (d, *J*(1',2') = 6.7, H_a-C(1'')); 6.40 (dd, *J*(1',2'') = 6.7, *J*(1',2') = 6.7, H_b-C(1'')); 7.59 (s, H_b-C(6)); 7.90 (d, *J*(5,6) = 8.0, H_a-C(6)). ¹³C-NMR (68 MHz, D₂O): 34.30; 38.95; 60.14; 65.28; 68.64; 70.56; 71.33; 80.26; 83.79; 83.88; 85.10; 85.22; 85.35; 87.42; 102.45; 111.57; 136.17; 141.54; 151.28; 151.52; 164.50; 166.09; 171.69. ³¹P-NMR (109 MHz, D₂O): 0.56.

{5'-2'-O-[Methyleneimino(2-oxoethane-2,1-diyl)]-Linked 5'-O-(4,4'-Dimethoxytrityl)-P-thiouridyl-(3' → 5')-2'-deoxyuridine S-Phenyl Ester (**16**). A soln. of **13** (350 mg, 0.29 mmol) in 80% AcOH (5 ml) was stirred for 5 h. The mixture was evaporated and the remaining AcOH removed by repeated co-evaporations with EtOH. The residue was rendered anhydrous by repeated co-evaporations with anh. pyridine and then dissolved in anh. pyridine (9 ml). 4,4'-Dimethoxytrityl chloride (268 mg, 0.78 mmol) was added, and the soln. was stirred for 20 h. The mixture was partitioned between CHCl₃ (20 ml) and sat. aq. NaHCO₃ soln. (20 ml), the org. phase washed 3 times with sat. aq. NaHCO₃ soln., dried (Na₂SO₄), and evaporated and the residue submitted to CC (silica gel, CHCl₃/MeOH 100:2): **16** (250 mg, 78%). ¹H-NMR (270 MHz, D₂O): 1.98 (m, H_b'-C(2')); 2.38 (m, H_b-C(2')); 3.30 (m, H_a'-C(5'')); 3.50 (m, H_a-C(5'')); 3.73 (s, 2 MeO); 3.90 (m, H_b-C(4'')); 4.00–4.10 (m, 2 H, H_a-C(4'), CH₂N); 4.10–4.60 (m, 7 H, 2 H_b-C(5'), H_b-C(3'), H_a-C(2'), CH₂N, OCH₂C); 5.24

(*m*, H_a–C(3')); 5.27 (*d*, $J(5,6) = 7.9$, H_a–C(5)); 6.00 (*d*, $J(1',2') = 5.9$, H_a–C(1')); 6.20 (*t*, $J(1',2') = J(1',2'') = 5.9$, H_b–C(1')); 7.62 (*d*, $J(5,6) = 7.9$, H_a–C(6)); 7.83 (*t*, $J(6,CH_2) = 3.9$, H_b–C(6)). ¹³C-NMR (68 MHz, CDCl₃): 34.25; 34.36; 40.45; 55.01; 55.04; 61.83; 67.84; 67.96; 69.33; 69.76; 70.01; 80.94; 81.76; 81.89; 83.76; 84.17; 84.30; 85.30; 85.88; 87.31; 87.57; 103.02; 111.38; 111.73; 112.81; 113.14; 123.68; 123.76; 123.86; 127.08; 127.28; 127.85; 127.92; 127.96; 129.60; 129.63; 129.78; 129.83; 129.97; 134.09; 134.29; 134.34; 134.47; 134.67; 134.72; 134.79; 138.98; 139.26; 143.47; 143.76; 150.15; 150.24; 150.49; 158.56; 158.69; 162.77; 163.34; 168.63; 168.70; 168.98. ³¹P-NMR (109 MHz, D₂O): 25.64; 24.85. Anal. calc. for C₄₈H₄₈N₅O₁₅PS · 2H₂O: C 55.76, H 5.07, N 6.77; found: C 55.26, H 4.92, N 6.23.

[5'-2'-O-[Methyleneimino(2-oxoethane-2,1-diyl)]-Linked 5'-O-(4,4'-Dimethoxytrityl)-P-thiouridyl-(3' → 5')-2'-deoxyuridine 3'-(2-Cyanoethyl Diisopropylphosphoramidite) S-Phenyl Ester (**17**). Compound **16** (200 mg, 0.18 mmol) was rendered anhydrous by repeated co-evaporations with anhydrous pyridine and toluene. The residue was dissolved in anhydrous CH₂Cl₂ (2 ml). To this solution were added ¹Pr₃EtN (39 μl, 0.22 mmol) and 2-cyanoethyl diisopropylphosphoramidochloridite (48 μl, 0.22 mmol), and the resulting mixture was stirred for 1 h. The mixture was diluted with CH₂Cl₂ (20 ml), the solution washed 3 times with saturated aqueous NaHCO₃ solution (20 ml), dried (Na₂SO₄), and evaporated and the residue submitted to CC (silica gel, hexane/AcOEt 1 : 4 containing 1% pyridine): **17** (180 mg, 71%). ¹H-NMR (270 MHz, D₂O): major isomer: 1.30 (*m*, 4 Me); 2.10 (*m*, H'_b–C(2')); 2.40–2.80 (*m*, CH₂CN, H_b–C(2')); 3.20 (*m*, H'_a–C(5')); 3.50–3.98 (*m*, 2 MeO, H_a–C(4'), H_a–C(5'), CH₂O, NCH); 4.00–4.78 (*m*, H_a–C(2'), CH₂N, CH₂CO, H_b–C(4'), H_b–C(3'), 2H_b–C(5')); 4.91 (*m*, H_a–C(2')); 5.37 (*d*, $J(5,6) = 8.2$, H_a–C(5)); 6.18 (*m*, H_a–C(1')); 6.28 (*t*, $J(1',2') = J(1',2'') = 6.3$, H_b–C(1')); 6.90 (*m*, 4 arom. H); 7.20–7.82 (*m*, 14 arom. H); 7.60 (*m*, H_a–C(6), H_b–C(6)); 9.01–9.80 (br., NH); minor isomer: 7.80 (*d*, H_a–C(6)); 6.40 (*t*, $J(1',2') = J(1',2'') = 5.6$, H_b–C(1')); 6.00 (*m*, H_a–C(1')). ¹³C-NMR (68 MHz, CDCl₃): 20.29; 20.40; 21.39; 24.53; 34.50; 39.12; 39.93; 43.22; 43.40; 55.26; 57.92; 58.04; 58.19; 58.33; 62.12; 67.87; 69.87; 70.42; 73.17; 73.48; 74.25; 81.51; 81.98; 83.88; 84.35; 85.82; 87.46; 87.75; 102.75; 103.34; 111.64; 111.73; 112.31; 113.30; 113.37; 117.62; 117.74; 124.31; 124.42; 125.23; 127.28; 127.46; 128.10; 128.97; 129.76; 130.12; 133.96; 134.41; 134.52; 134.68; 134.74; 134.90; 134.95; 138.92; 143.59; 143.90; 150.06; 150.12; 150.57; 152.06; 150.12; 150.57; 152.06; 158.76; 158.87; 162.05; 162.26; 162.71; 163.07; 168.19; 168.50. ³¹P-NMR (109 MHz, D₂O): 24.78; 24.86; 25.01; 149.69; 150.10; 150.35; 150.44. Anal. calc. for C₅₇H₆₅N₇O₁₆P₂S · 5/2 H₂O: C 55.07, H 5.68, N 7.88; found: C 54.89, H 5.34, N 7.84.

Centrally [5'-2'-O-[Methyleneimino(2-oxoethane-2,1-diyl)]-Linked Thymidyl-(3' → 5')-uridyl-(3' → 5')-2'-deoxyuridyl-(3' → 5')-thymidine (**18**). A commercially available DM[(MeO)₂Tr]T-loaded CPG support (41 mg, 1 mmol) was placed in a glass column equipped with a glass filter, a stopper, and a stopcock. The (MeO)₂Tr group was removed by treatment with 1% CF₃COOH in CH₂Cl₂ (2 ml × 2) several times. After the support was washed with CH₂Cl₂ (10 ml), the 5'-hydroxy group liberated was coupled with **17** (39 mg, 30 μmol) in the presence of 1*H*-tetrazole (21 mg, 0.3 mmol) in MeCN (200 μl) for 10 min under Ar. After the excess phosphoramidite unit and 1*H*-tetrazole were removed by washing with CH₂Cl₂ (10 ml), capping of the unreacted OH group with 0.2M Ac₂O in DMAP/pyridine 1 : 9 (2 ml) for 2 min, oxidation with 0.1M I₂ in H₂O/pyridine/THF 1 : 10 : 40 (2 ml) for 1 min, detritylation with 1% CF₃COOH in CH₂Cl₂ (2 ml × 5), and elongation of another thymidylate residue were carried out according to the standard protocol for the solid-phase oligonucleotide synthesis. After the (MeO)₂Tr group was removed by treatment with 1% CF₃COOH in CH₂Cl₂ (2 ml × 5), the removal of the alkali-labile protective groups and elution of the oligonucleotide were carried out by treatment with 0.5M NaOH/pyridine 1 : 1 (10 ml) for 30 min. The eluant was neutralized on Dowex 50W × 8 (H⁺ form, 3 ml), and the Dowex 50W × 8 residue was removed by filtration. The filtrate was evaporated and the residue lyophilized. The resulting white solid was purified by anion-exchange HPLC (*Fax*; linear gradient of 50 → 770 mM NaCl in 25 mM phosphate buffer (pH 6.0) for 50 min). After evaporation, the remaining salt was removed by CC (*Sephadex G-15*, H₂O). The eluant was lyophilized: **18** (6 A₂₆₀). ¹H-NMR (270 MHz, D₂O): 7.67 (*d*, $J(5,6) = 8.3$, H–C(6)); 7.68 (*s*, H–C(6) of T); 7.62 (*s*, H–C(6) of U); 7.50 (*s*, H–C(6) of dU); 6.30 (*m*, 2 H, H–C(1') of T); 6.10 (*d*, $J(1',2') = 5.0$, 1 H, H–C(1')); 5.90 (*d*, $J(5,6) = 8.3$, 1 H, H–C(5) of U); 1.86 (*s*, 1 Me); 1.87 (*s*, 1 Me). ³¹P-NMR (109 MHz, D₂O): 0.29; –0.29; –0.47.

General Procedure of the Synthesis of Oligothymidylates Containing the Cyclic-Dimer Unit **14**: T-T-T-T-(cUpdU)-T-T-T-T (**19**) and T-T-T-T-T-T-T-(cUpdU)-T-T-T-T-T-T (**20**). The fully protected oligothymidylates having the chain length of a 4-mer and 7-mer were prepared on an automated DNA synthesizer with the commercially available [(MeO)₂Tr]T-loaded CPG support (41 mg, 1 mmol) and the thymidine 3'-phosphoramidite unit. Then, the solid support was placed in a glass column equipped with a glass filter, a stopper, and a stopcock. The 5'-terminal (MeO)₂Tr group was removed by treatment with 1% CF₃COOH in CH₂Cl₂ (2 ml × 5), and the resin was washed with CH₂Cl₂ (10 ml). The 5'-hydroxy group liberated was coupled with the dimer unit **17** (39 mg, 30 μmol) in the presence of 1*H*-tetrazole (21 mg, 0.3 mmol) in MeCN (200 μl) for 10 min under

Ar. After the excess phosphoramidite unit and 1*H*-tetrazole were removed by washing with CH₂Cl₂ (10 ml), capping of the unreacted OH group with 0.12M AcOH in DMAP/pyridine 9 : 1 (2 ml) for 2 min, oxidation with 0.1M I₂ in H₂O/pyridine/THF 1 : 10 : 40 (2 ml) for 1 min was carried out. The solid support was put on an automated DNA synthesizer, and the remaining thymidylate sequences were constructed automatically. After all the couplings were achieved, the fully protected oligonucleotides were deprotected and eluted by treatment with 0.5M NaOH/pyridine 1 : 1 (10 ml) for 30 min. Then, the eluant was neutralized with Dowex 50W × 8 (pyridinium salt, 3 ml), and the Dowex resin was removed by filtration. To the filtrate was added Et₃N (5 ml), and the soln. was evaporated. The residue was placed on a Sep-Pak C₁₈ column, and the shorter oligothymidylates were washed out with H₂O (10 ml). The (MeO)₂Tr group of the desired oligothymidylates was removed by treatment with 3% CF₃COOH in CH₂Cl₂ (5 ml) on the column, and the deprotected oligothymidylates were eluted with the same solvent. The eluant was evaporated and the residue lyophilized. The resulting white solid was further purified by anion-exchange HPLC (Fax, linear gradient of 50 → 770 mM NaCl in 25 mM phosphate buffer (pH 6.0) for 50 min). After evaporation, the remaining salt was removed by CC (Sephadex G-15, H₂O). The eluant was lyophilized: **19** (6 A₂₆₀) or **20** (22 A₂₆₀).

19: t_R 24.3 min UV (H₂O): 262.8; min. 233.0.

20: t_R 30.5 min. UV (H₂O): 263.2; min. 233.2.

CD Spectra. Oligonucleotides were dissolved in 10 mM sodium phosphate (pH 7.0), and the absorbance at 264 nm was adjusted to 0.5. The soln. was placed in a 5-mm cell, and the spectra were accumulated 16 times at 20 nm/s scan speed. The baseline was corrected by the subtraction of the CD spectra of the solvent recorded under the same spectrometer conditions at 20°. The temp. was controlled by a Haake-C circulator, and the sample was equilibrated for 15 min after the cell holder had reached the desired temp. The spectra were displayed after having been smoothed by averaging. The concentration of the sample was calculated on the assumption that the ε₂₆₀ was 19600.

Measurement of the H,H-Coupling Constants in 1D-¹H-NMR Spectra. The cyclic dimer **14** (100 A₂₆₀) was dissolved in 10 mM sodium phosphate (700 μl, pH 7.0) and then lyophilized 3 times with 99.8% D₂O. The resulting white precipitate was dissolved in 700 μl of 99.95% D₂O. The peak of H₂O was suppressed by pre-saturation. The coupling constants were measured at the 0.15 Hz of digital resolution, accomplished by the spin-simulation deconvolution module of the spectrometer.

2D-NOESY Spectrum. Conditions: 2048 × 512 data points; mixing time 700 ms; data zero-filled to 2048 in the f₁ direction before Fourier transformation.

Polyacrylamide-Gel Electrophoresis. A soln. of 0.1 A₂₆₀ units of **19**, T₁₀, or T₁₁ in formamide (3 μl) was charged on a 20% polyacrylamide gel plate containing 7M urea (30 × 38 cm) containing 90 mM Tris-boric acid, and 3 mM EDTA for 2 h with 90 mM Tris-borate buffer at 1500 V. The gel was visualized by 0.2% toluidine blue in 0.4M KOAc (pH 4.8) and dried for 5 h under reduced pressure. The mobilities observed were 11.1, 11.4, and 11.1 cm for **19**, T₁₀, and T₁₁, resp.

Molecular Modeling by Molecular-Mechanics Calculation. Conformation search and energy minimization were carried out by MacroModel V.4.5 running on a Silicon-Graphics-Indigo-2 workstation. The initial structure was constructed from the nucleotide-unit structure extracted from either the typical A-type or B-type DNA duplex. Four calculation runs were carried out in which the ribose moieties of the 5'-terminal and 3'-terminal nucleoside unit were fixed in the {N-type and N-type}, {N-type and S-type}, {S-type and N-type}, and {S-type and S-type} conformations, resp. In the conformation search, 5000 conformers were selected in the MCMM mode, in which the conformers were generated randomly, and they were energy-minimized by the AMBER* united atom force. The low-energy structures having energy within 20 kJ/mol from the lowest energy were selected and subjected to further energy minimization by the AMBER* all-atom force. In all simulations, dielectric constant ε 1.0 and the GB/SA solvent model were used.

UV Melting Curves. Oligothymidylate (5 μmol) and oligodeoxyadenylates (5 μmol) were dissolved in 2 ml of 10 mM sodium phosphate and 150 mM NaCl (pH 7.0). The mixture was heated to 90° and then cooled to 0° within 90 min. After the mixture was equilibrated at 0° for 20 min, the UV absorbance at 260 nm was recorded as the temp. was raised at the rate of 1°/min.

REFERENCES

- [1] H. M. Wu, D. M. Crothers, *Nature (London)* **1984**, 308, 509; C. A. Frederick, J. Grable, M. Melia, C. Samudzi, L. Jen-Jacobson, B.-C. Wang, P. Green, H. W. Boyer, J. M. Rosenberg, *ibid.* **1984**, 309, 327; A. K. Aggarwal, D. W. Rodgers, M. Drottar, M. Ptashne, S. C. Harisson, *Science (Washington, D.C.)* **1988**, 242,

- 899; I. Husain, J. Griffith, A. Sancer, *Proc. Natl. Acad. Sci. U.S.A.* **1988**, *85*, 2558; R. G. Brennan, S. L. Roderick, Y. Takeda, B. W. Matthews, *ibid.* **1990**, *87*, 8165; D. B. Nicolov, H. Chen, E. D. Halay, A. A. Usheva, K. Hisataka, D. K. Lee, R. G. Roeder, S. K. Burley, *Nature (London)* **1990**, *377*, 119; C. I. Wang, J. S. Taylor, *ibid.* **1991**, *88*, 9072; S. C. Schultz, G. C. Shields, T. A. Steitz, *Science (Washington, D.C.)* **1991**, *253*, 1001; J. L. Kim, D. B. Nikolov, S. K. Burley, *Nature (London)* **1993**, *365*, 520; Y. Kim, J. H. Geiger, S. Hahn, P. B. Sigler, *ibid.* **1993**, *365*, 512; for recent studies on DNA binding, see P. A. Rice, S. Yang, K. Mizuuchi, H. A. Nash, *Cell (Cambridge, Mass.)* **1996**, *87*, 1295; F. Pio, R. Kodandapani, C. Z. Ni, W. Shepard, M. Klemsz, S. R. McKercher, R. A. Maki, K. R. Ely, *J. Biol. Chem.* **1996**, *271*, 23329; K. Swaminathan, P. Flynn, R. J. Reece, R. Marmorstein, *Nat. Struct. Biol.* **1997**, *4*, 751, F. J. Meyer-Almes, D. Porschke, *J. Mol. Biol.* **1997**, *269*, 842; N. Rajaram, T. K. Kerppola, *EMBO J.* **1997**, *16*, 2917; P. Brownlie, T. Ceska, M. Lamers, C. Romier, G. Stier, H. Teo, D. Suck, *Structure (London)* **1997**, *5*, 509; C. M. Nunn, E. German, S. Neidle, *Biochemistry* **1997**, *36*, 4792; C. R. Escalante, J. Yie, D. Thanos, A. K. Aggarwal, *Nature (London)* **1998**, *391*, 103; C. J. Squire, G. R. Clarke, W. A. Denny, *Nucleic Acids Res.* **1997**, *25*, 4072; D. A. Leonard, N. Rajaram, T. K. Kerppola, *Proc. Natl. Acad. Sci. U.S.A.* **1997**, *94*, 4913.
- [2] H. W. Pley, K. M. Flaherty, D. B. McKay, *Nature (London)* **1994**, *372*, 68; W. G. Scott, J. T. Finch, A. Klug, *Nucleic Acids Symp. Ser.* **1995**, *34*, 214; W. G. Scott, J. T. Finch, A. Klug, *Cell (Cambridge, Mass.)* **1995**, *81*, 991; W. G. Scott, J. B. Murray, J. R. P. Arnold, B. L. Stoddard, A. Klug, *Science (Washington, D.C.)* **1996**, *274*, 2065; S. T. Sigurdsson, F. Eckstein, *Trends-Biotechnology* **1995**, *13*, 286.
- [3] G. J. Quigley, A. Rich, *Science (Washington, D.C.)* **1976**, *194*, 796.
- [4] K. Seio, T. Wada, K. Sakamoto, S. Yokoyama, M. Sekine, *J. Org. Chem.* **1996**, *61*, 1500.
- [5] K. Seio, T. Wada, K. Sakamoto, S. Yokoyama, M. Sekine, *J. Org. Chem.* **1998**, *63*, 1429.
- [6] a) A. Kamp, C. J. Pillar, W. J. Woodford, M. P. Mertes, *J. Med. Chem.* **1976**, *19*, 900; b) G. T. Shiau, R. F. Schinazi, M. S. Chen, W. H. Prusoff, *ibid.* **1980**, *23*, 127.
- [7] M. Sekine, L. S. Peshakova, T. Hata, unpublished work.
- [8] J. C. Sheehan, P. A. Cruickshank, G. L. Boshart, *J. Org. Chem.* **1961**, *26*, 2525; J. C. Sheehan, J. J. Hlavka, *ibid.* **1956**, *21*, 439.
- [9] M. Sekine, J. Matsuzaki, T. Hata, *Tetrahedron* **1985**, *41*, 5279.
- [10] M. D. Matteucci, M. H. Caruthers, *J. Am. Chem. Soc.* **1981**, *103*, 3185.
- [11] S. L. Beaucage, *Tetrahedron Lett.* **1984**, *25*, 375; M. F. Moore, S. L. Beaucage, *J. Org. Chem.* **1985**, *50*, 2019.
- [12] J. Brahm, J. C. Maurizot, A. M. Michelson, *J. Mol. Biol.* **1967**, *25*, 481; C. Cantor, M. M. Warshaw, H. Shapiro, *Biopolymers* **1970**, *9*, 1059.
- [13] C. Altona, M. Sundaralingam, *J. Am. Chem. Soc.* **1972**, *94*, 8205; H. A. Gabb, S. C. Harvey, *ibid.* **1993**, *115*, 4218; M. Levitt, A. Warshal, *ibid.* **1978**, *100*, 2607.
- [14] M. Sundaralingam, *Biopolymers* **1969**, *7*, 821.
- [15] D. B. Davis, *Prog. Nucl. Magn. Res. Spectrosc.* **1978**, *12*, 135.
- [16] D. B. Davies, S. S. Danyluk, *Biochemistry* **1974**, *13*, 4417.
- [17] M. Lipton, W. C. Still, *J. Comput. Chem.* **1988**, *9*, 343.
- [18] S. J. Weiner, P. A. Kollman, D. A. Case, U. C. Singh, C. Ghio, G. Alagona, S. Profeta, Jr., P. Weiner, *J. Am. Chem. Soc.* **1984**, *106*, 765; S. J. Weiner, P. A. Kollman, D. T. Nguyen, D. A. Case, *J. Comput. Chem.* **1986**, *7*, 230; D. Q. McDonald, W. C. Still, *Tetrahedron Lett.* **1992**, *33*, 7743.
- [19] W. C. Still, A. Tempczyk, R. C. Hawley, T. Hendrickson, *J. Am. Chem. Soc.* **1990**, *112*, 6127.
- [20] D. G. Gorenstein, *Chem. Rev.* **1994**, *94*, 1315; V. A. Roongta, C. R. Jones, D. G. Gorenstein, *Biochemistry* **1990**, *29*, 5245; C. Karlake, M. V. Botuyan, D. G. Gorenstein, *ibid.* **1992**, *31*, 1849; D. G. Gorenstein, K. Lai, D. O. Shah, *ibid.* **1984**, *23*, 6717; P. K. Kline, L. G. Marzilli, D. Live, G. Zon, *Biochem. Pharmacol.* **1990**, *40*, 97; E. M. Goldfield, B. A. Luxon, V. Bowie, D. G. Gorenstein, *Biochemistry* **1983**, *22*, 3336.
- [21] J. C. Marine, S. D. Levene, D. M. Crothers, P. T. Englund, *Proc. Natl. Acad. Sci. U.S.A.* **1982**, *79*, 7664; T. E. Haran, D. M. Crothers, *Biochemistry* **1989**, *28*, 2763; M. Shatzky-Schwartz, Y. Hiller, Z. Reich, R. Ghirlando, S. Weinberger, A. Minsky, *ibid.* **1992**, *31*, 2339, and refs. cit. therein.
- [22] W. Saenger, 'Principle of Nucleic Acid Structure', Springer-Verlag, New York, 1978.

Received August 24, 1999